Appl Magn Reson (2016) 47:335–347
DOI 10.1007/s00723-015-0759-z

Applied
Magnetic Resonance

Self-diffusion of Water and Blood Lipids in Mouse Erythrocytes

Irina A. Avilova[1] · Anastasiya V. Smolina[1] · Alexander I. Kotelnikov[1] · Raisa A. Kotelnikova[1] · Valentin V. Loskutov[3] · Vitaly I. Volkov[1,2]

Received: 17 September 2015 / Revised: 23 November 2015 / Published online: 6 January 2016

Abstract The self-diffusion of water and lipids in water—mouse RBCs' suspension was investigated by pulsed field gradient NMR technique at different diffusion times in temperature range from 5 to 35 °C. For the experimental data interpretation, the phenomenological scaling approach was applied. The intracellular water restriction size (2.1 μm), erythrocyte water permeability (about 10^{-5} m/s), intracellular residence time (about 20 ms), and water permeability activation energy (24.1 ± 1.9 kJ/mol) were calculated. The lipid self-diffusion coefficients are varied from 3×10^{-12} to 10^{-11} m^2/s depending on temperature and diffusion time. The lipid lateral self-diffusion activation energy is about 25 ± 2.9 kJ/mol.

1 Introduction

The molecular and ionic exchange in biological cells is the main metabolism process in life form. Diffusive transport of water and functional substances in the presence of permeable erythrocyte membranes (RBCs) is of fundamental biological importance. Pulsed NMR techniques are the methods of choice for the molecular exchange process investigations in RBCs [1–24]. The first water exchange rate NMR measurements between intra- and extracellular water are started since the beginning of 70th in the last century. There are two ways of the intracellular water residence time measurements: paramagnetic doping and pulsed field gradient NMR

✉ Vitaly I. Volkov
vitwolf@mail.ru

[1] Institute of Problems of Chemical Physics RAS, Academician Semenov Avenue, 1, Chernogolovka, 142432 Moscow Region, Russia

[2] Science Center in Chernogolovka RAS, Lesnaya str., 9, Chernogolovka, 142432 Moscow Region, Russia

[3] Mari State University, Lenin sq., 1, Mari El, 424000 Yoshka-Ola, Russia

techniques (PFG NMR). In the first case, the paramagnetic (manganese or gadolinium) salt solutions are injected in the extracellular water area [1–12]. The exchange rate $k = 1/\tau$ is calculated as the difference between extra- and intracellular water proton spin relaxation rates and the permeability as $P = k \cdot V/S$ is calculated, where τ is intracellular water residence time and V/S is the cell volume to surface ratio [4]. The main disadvantage of this elegant way of water permeability measurement is the existence of paramagnetic ions in the biological systems that may influence the real exchange process. From this point of view, the pulsed field gradient technique is much more preferable [25]. This technique enables to measure the apparent intra- and extracellular water self-diffusion coefficients and intra- and extracellular water relative amount [5, 13–24]. The measured diffusion coefficient, $D_s(t_d)$, depends on observation diffusion time t_d and is a sensitive function of membrane permeability, cell shape and size. Erythrocyte red blood cells (RBCs) are ideally suited for these studies since the cell size and permeability may be independently controlled.

The PFG NMR investigations were carried out for human and more than 30 different species RBCs. The analysis of spin-echo signal attenuation decay (diffusion decay) shape dependence on the diffusion time is more productive [5, 13–24, 26–32]. On the short time scale, the dependence $D_s(t_d)$ is characterized by the surface-to-volume ratio (S/V). For the simplest models, the relation between $D_s(t_d)$ and S/V is given in [33–35].

In the intermediate or long time region for the real systems with the permeability for the $D_s(t_d)$ approximation, the scaling approach may be applied [30–32, 36]. From the scaling approach equations, it is possible to calculate permeability and restriction size. The intracellular water residence time τ may be calculated from the dependence of apparent intracellular water amount (population) on diffusion time. Therefore, PFG NMR is a unique technique for the direct permeability and restriction size measurement. From the point of view of experimental results' interpretation, the phenomenological scaling approach is very attractive. The applicability of this method was confirmed for chlorella [30] and yeast [31, 32] cells' water suspension. The scaling approach has not been applied for RBCs' suspension because the detailed experimental data of spin-echo attenuation in 3–4 orders of magnitude for the wide interval of diffusion times are absent. Another reason is the diffraction shape of diffusion decays for any species [2, 3, 16, 21, 22, 24]. As it was mentioned above, the RBCs' suspensions of many exotic species were investigated by NMR. The mouse RBCs' NMR investigation is almost unknown, in spite of the fact that mice are widely used for different medical and biological testing.

The aim of the proposal paper is the detailed investigation of water exchange in mouse red blood water suspension by PFG NMR at different temperatures. The attention also will be paid to the blood lipid self-diffusion.

2 Experimental (Materials and Methods)

2.1 Object

Mouse red blood cells were investigated. The blood sampling was made from narcotazed mice by means of decapitation. The 0.11-M sodium citrate aqueous solution is used as anticoagulant. The citrate solution to blood ratio was 1 to 5.

The blood was centrifuged during 15 min at 1000 rounds per minute. The plasma was decanted. The erythrocyte sediment was resuspended in isotonic NaCl solution (0.85 % NaCl solution contained 5 mmol buffer Na-phosphate, pH = 7.4). The centrifugation and decantation were triply repeated, the second and third centrifugation duration were 7 min. The fresh NaCl isotonic solution for the following resuspended procedure was used. The erythrocyte sediment stored in refrigerator at 4 °C no more than 36 h. The sediment was settled during 3 h before NMR measurements. The temperature was decreased from 35 to 5 °C and the samples were thermostated during 20 min at each temperature in transition.

2.2 Methods

The self-diffusion coefficients were measured on ^{1}H nuclei by pulsed field gradient technique at the frequency 400.22 MHz. The measurements were carried out on Bruker Avance-III—400 NMR spectrometer, equipped with the diff60 gradient unit. The pulsed field gradient stimulated echo sequence shown in Fig. 1 was used. Three 90° pulses produce a stimulated spin-echo at time $2\tau + \tau_1$ (where τ is the time interval between the first and second 90° pulses and τ_1—interval between the second and the third pulses). The magnetic field gradient pulses of amplitude g and duration δ were applied after the first and third 90° pulses. The gradient strength was varied linearly in 64 steps within a range from 0.1 to 27 *T/m* value. The integrated

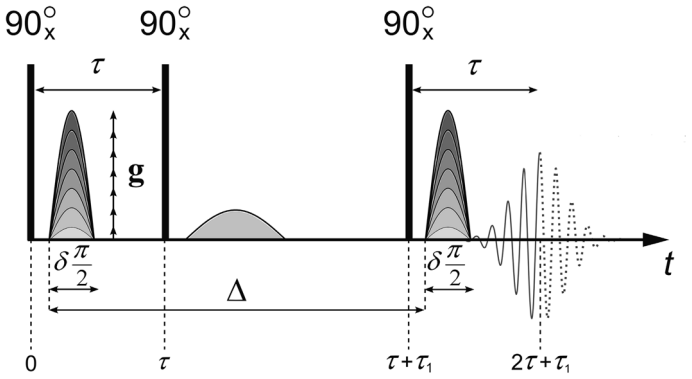

Fig. 1 Stimulated echo pulse sequence with the magnetic field gradient pulses. Here, τ is the time interval between the first and second RF pulses, τ_1 is the time interval between the second and the third ones. Δ is the interval between the gradient pulses, δ is duration of the equivalent rectangular magnetic field gradient pulses, g is the amplitude of the magnetic field gradient pulse and g_0 is the amplitude of the constant magnetic field gradient

intensities of spectrum lines were used to obtain the dependence of echo sign at attenuation on g^2 (diffusion decay) [30, 32, 37–39].

For the molecules undergoing unhindered isotropic Brownian motion, the evolution of spin-echo signal is described by the following equation.

$$A(2\tau, \tau_1, g) = A(2\tau, \tau_1, 0)\exp\left(-\gamma^2 g^2 \delta^2 t_d D_s\right), \quad (1)$$

where γ is gyromagnetic or magnetogyric ratio, $t_d = \Delta - \delta/3$ is the diffusion time, and D_s is the self-diffusion coefficient, and τ, τ_1 and g are shown in Fig. 1. $A(2\tau, \tau_1, 0)$ is expressed by the equation

$$A(2\tau, \tau_1, 0) = \frac{A(0)}{2}\exp\left(-\frac{2\tau}{T_2} - \frac{\tau_1}{T_1}\right), \ldots$$

where $A(0)$ is the signal intensity after the first radio frequency (RF) pulse (Fig. 1). T_1 and T_2 are the spin–lattice and spin–spin relaxation times, respectively. During measurement of echo signal evolution, τ and τ_1 are fixed, and only the dependence of A on g is analyzed, which is called the diffusion decay.

The erythrocytes' (RBCs) water suspension ^{1}H spectra at different values of pulsed field gradient amplitudes are shown in Fig. 2. The more intense signal in Fig. 2a (the chemical shift is 4.7 ppm) belongs to water molecules, the weak signals which are well distinguished at high-gradient pulsed amplitude are due to RBCs membrane. The more intensive signals belong to $(CH_2)_n$ and CH_3 lipid groups (chemical shifts about 1.4 and 0.8 ppm, correspondingly) [40]. The signals in the region 6–9 ppm due to RBCs protein components (aromatic, N–H and O–H groups, for example) [41]. Since the main aim is investigation of the self-diffusion of lipid, we analyzed diffusion decays of signals of lipid in the region 0–2 ppm.

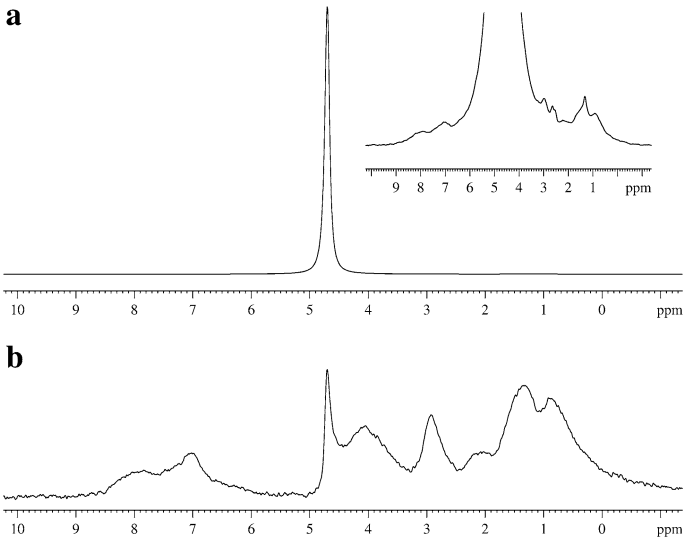

Fig. 2 The mouse erythrocytes' (RBCs) water suspension ^{1}H spectra with suppression of water signal pulsed field gradient amplitude $g = 0.375$ *T/m* − *a* and $g = 10.5$ *T/m* − *b*

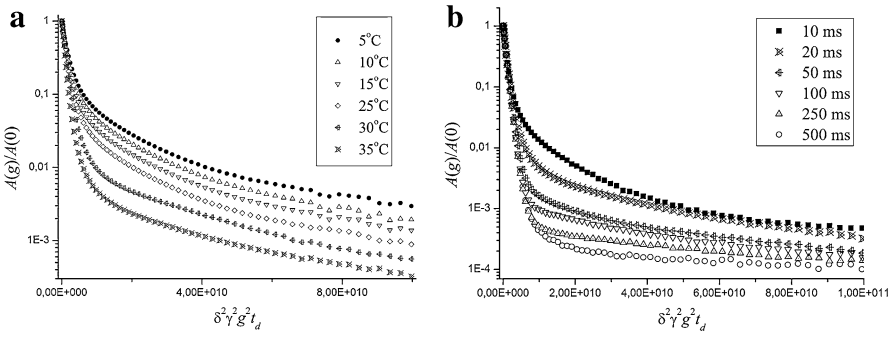

Fig. 3 The diffusion decays of water molecules in the mouse RBCs measured at various temperatures (**a** $T = 5$, 10, 15, 25, 30, and 35 °C; $t_d = 20$ ms) and diffusion times (**b** $t_d = 10$, 20, 50, 100, 200 and 500 ms; $T = 35$ °C)

The diffusion decays of ^{1}H water and $(CH_2)_n$ and CH_3 groups NMR spin-echo signals were analyzed.

The typical diffusion decays obtained at various diffusion times t_d and temperatures are shown in Fig. 3.The diffusion decay cannot be described by a single exponential function. In this case, the experimental curves

$$A(g) = \frac{A(2\tau, \tau_1, g)}{A(2\tau, \tau_1, 0)}$$

are usually decomposed into the exponential components, which are described by Eq. (1). For the multiphase system consisting of m phases in the case of slow (compare tot_d) molecular exchange between phases,

$$A(g) = \sum_{i=1}^{m} p_i' \exp(-\gamma^2 g^2 \delta^2 t_d D_{si}) \tag{2}$$

where D_{si} is the self-diffusion coefficient of ith component and

$$p_i' = p_i \exp\left(-\frac{2\tau}{T_{2i}} - \frac{\tau_1}{T_{1i}}\right) \Bigg/ \sum_{i=1}^{m} p_i \exp\left(-\frac{2\tau}{T_{2i}} - \frac{\tau_1}{T_{1i}}\right), \quad \sum_{i=1}^{m} p_i = 1.$$

Here, p_i is the relative amount of nuclei belonging to the molecules characterized by the self-diffusion coefficient D_{si}. The value p_i is called the population of ith phase. For the long T_1 and T_2 values, it is usually deduced that $p_i \approx p'_i$.

The detail of the curve decomposition on exponential diffusion decays is described in the references [42].

3 Results and Discussion

3.1 Water Self-Diffusion

The example of typical ^1H diffusion decay of water molecules in erythrocytes is shown in Fig. 4. This decay was decomposed on three exponential components,

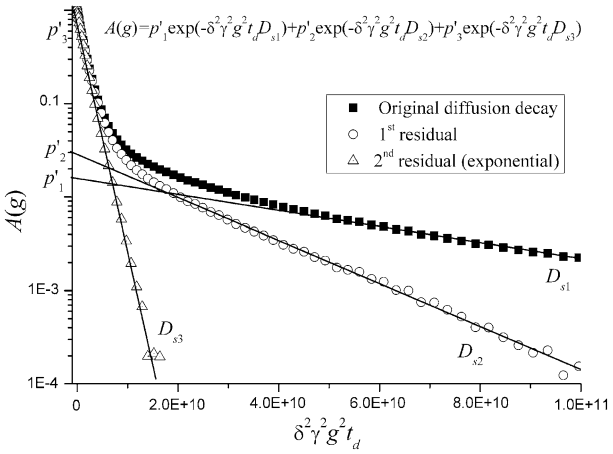

Fig. 4 The diffusion decay of water molecules in the mouse red blood cells at 5 °C for diffusion time $t_d = 50$ ms. The procedure of decomposition of the original diffusion decay on three exponential components according to Eq. (2) is shown: $D_{s3} = 0.6 \times 10^{-9}$ m^2/s, $p'_3 = 0.947$; $D_{s2} = 0.76 \times 10^{-10}$ m^2/s, $p'_2 = 0.045$; $D_{s1} = 1.37 \times 10^{-11}$ m^2/s, $p'_1 = 0.008$

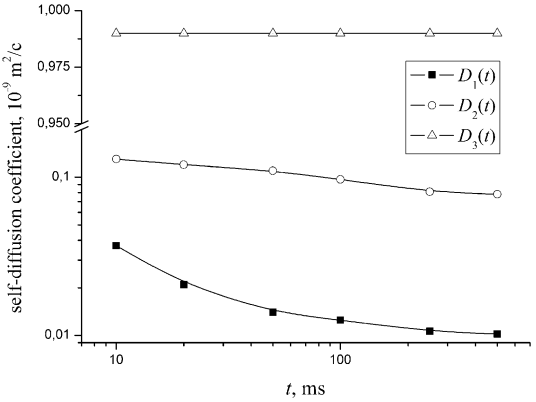

Fig. 5 The water self-diffusion coefficient D_{s1}, D_{s2} and D_{s3} dependences on the diffusion time t_d at 35 °C

which were characterized by self-diffusion coefficients D_{s1}, D_{s2}, D_{s3} and populations p_1, p_2, p_3. The analysis of diffusion decay curves at different diffusion times t_d shows that the values of populations p_1, p_2 and self-diffusion coefficients D_{s1}, D_{s2} depend on diffusion time t_d.

The dependences of D_{s1}, D_{s2} and D_{s3} on the diffusion time t_d are shown in Fig. 5.

The self-diffusion coefficients D_{s1} and D_{s2} decreased with increasing t_d, but for self-diffusion coefficient D_{s3}, which is close to the self-diffusion coefficient of bulk water, there is no dependence on td (Fig. 5). The populations p_1 and p_2 decreased, but population p_3 increased with increasing diffusion time t_d (Fig. 6). Three types of water in biological cell suspension are related to the bulk water, the extracellular water and the intracellular water, correspondingly [30–32]. In our discussion, the main attention will be paid to the intracellular water behavior, which is characterized by D_{s1} and p_1.

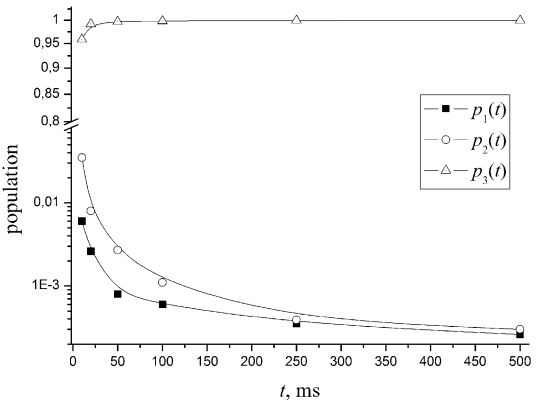

Fig. 6 The population p_1, p_2 and p_3 dependences on the diffusion time t_d at 35 °C

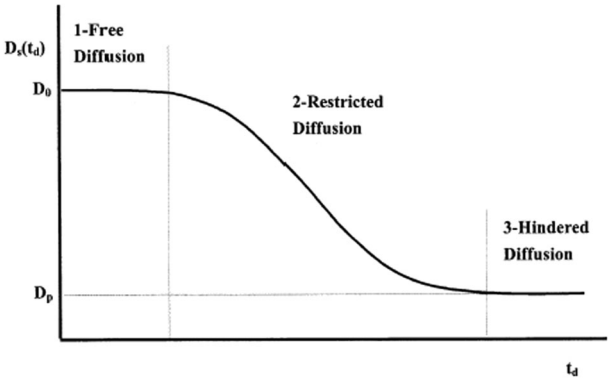

Fig. 7 Idealized dependence of liquid self-diffusion coefficient D_s on diffusion time in the pore systems with permeable walls

The decreasing of water self-diffusion coefficients with the increasing of diffusion time indicates that water diffusion in mouse RBCs is restricted. It is well known that dependence of water molecule diffusion coefficients on t_d in pore systems and biological cells shows S-shape, as shown in Fig. 7 [30, 31, 43–45]. There are three parts of this S-shaped curve. The region 1 is the free diffusion region, where D_0 is non-restricted self-diffusion coefficient at $t_d \to 0$.

The region of restricted diffusion (region 2) is where the averaging of local water translation motions over a large enough volume does not occur yet. The region of hindered diffusion (region 3) is where the effect of total averaging of interpore diffusion is achieved due to permeability of pore walls. In this region (so-called long time diffusion regime, $D_p = \lim_{t_d \to \infty} D(t_d)$) water self-diffusion coefficient D_p is also independent of t_d and

$$\frac{1}{D_p} = \frac{1}{D_0} + \frac{1}{Pa} \tag{3}$$

where P is permeability of pore (or cell) wall, and a is the wall (or cell) size [30–32].

The dependencies $D_s(t_d)$, related to intercellular water, contain information about cell size, cell shapes and cell wall permeability. The key problem is to extract these characteristics from $D_s(t_d)$ dependences. From Einstein equation, the water molecule displacement ‹a› is $(6D_st_d)^{1/2}$. The region of restricted diffusion (region 2) consists of two parts. On the short time scale, when the molecule displacement is $6D_0t_d \ll \langle a^2 \rangle$, $D_s(t_d)$ is characterized by the surface-to-volume ratio (S/V). For the simplest models, the relation between $D_s(t_d)$ and S/V is given by Eq. (4) [33]

$$D(t_d) = D_0\left(1 - \frac{4}{9\sqrt{\pi}}\frac{S}{V}\sqrt{D_0t_d}\right). \tag{4}$$

However, in some cases, the ratio S/V is not sufficiently informative parameter. In [34, 35], the expression (5) for the time dependence of the liquid self-diffusion coefficient in a porous medium was obtained where the diffusion coefficient is an exponential function of cell size a:

$$D(t_d) = \left(D_0 - D_p\right)\exp\left(-\frac{7.8\sqrt{D_0t_d}}{a}\right) + D_p. \tag{5}$$

Equation (5) satisfactorily describes the time dependence of the self-diffusion coefficient for media with high permeability. In systems with low permeability (for instance, the self-diffusion in cells), solution Eq. (5) at intermediate diffusion regime deviates from the experimental values [46].

In the intermediate or long time part for the non-permeable pore or cell walls

$$D_s(t_d) = \frac{\langle a^2 \rangle}{6t_d}. \tag{6}$$

For the real systems, the permeability exists and the slope of $D_s(t_\mathrm{d})$ is less than t_d^{-1}. This situation was analyzed in detail in [30–32, 36], where the scaling approach was applied for $D_s(t_\mathrm{d})$ analysis. The restriction size a may be calculated from the dependence-effective self-diffusion coefficient $D_s^{\mathrm{eff}}(t_\mathrm{d})$, which reads t_d as proportional to t_d^{-1} which is taking place for the non-permeable pores. The $D_s^{\mathrm{eff}}(t_\mathrm{d})$ is given by the following equation [30, 31]

$$D_s^{eff}(t_d) = \frac{D_s(t_d) - D_p}{D_0 - D_s(t_d)} \cdot D_0, \tag{7}$$

where $D_s(t_\mathrm{d})$ is the experimental dependence of self-diffusion coefficient on t_d. The dependences of $D_s(t_\mathrm{d})$ and $D_s^{eff}(t_\mathrm{d})$ on diffusion time t_d at different temperatures are shown in Fig. 8a, b. The physical meaning of D_o and D_p is clear from the Fig. 7 explanation.

As shown in Fig. 8b, $D_s^{\mathrm{eff}}(t_\mathrm{d})$ is proportional to t_d^{-1} starting from 20 ms. $D_s^{eff}(t_d)$ does not depend on temperature. It means that restriction sizes are the same at different temperatures. The size of diffusion restriction a calculated from Eq. 6 is 2.1 μm. The a value does not depend on temperature and is in agreement with the half of narrow size [2].

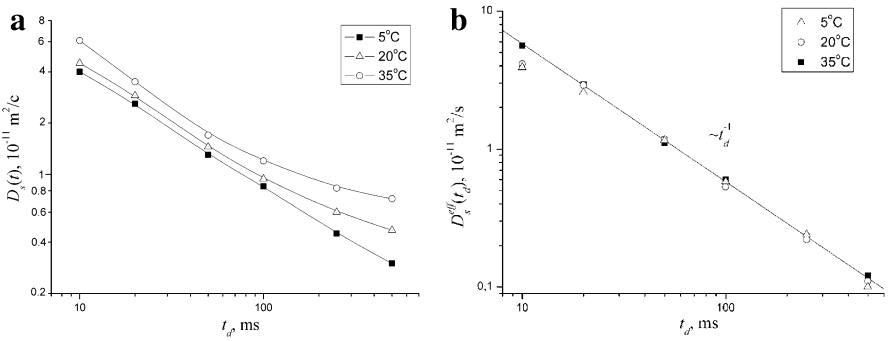

Fig. 8 The experimental dependence of self-diffusion coefficients $D_s(t)$ (**a**) and effective self-diffusion coefficients $D_s^{eff}(t_d)$ on the diffusion time t_d as calculated from Eq. 7 (**b**) for intracellular water molecules in the mouse RBCs. The temperatures of measurements are 5, 20 and 35 °C. *Solid straight line* in **b** is proportional $\sim t_d^{-1}$

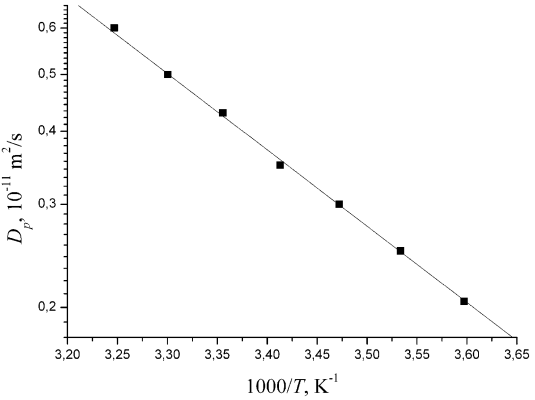

Fig. 9 The temperature dependence of the hindered water self-diffusion coefficients D_p. The *solid straight line* is the Arrhenius equation approximation. The activation energy is 24.1 ± 1.9 kJ/mol

The values of hindered self-diffusion coefficients D_p were also calculated from Eq. (7). The temperature dependence of D_p is shown in Fig. 9.

This dependence may be approximated by Arrhenius equation. The activation energy value is 24.1 ± 1.9 kJ/mol which is close to literature data for mouse RBCs [11]. Keeping in mind that D_o is larger compared to D_p (for instance, D_p is 7×10^{-12}m^2/s and D_o is 4×10^{-11}m^2/s at 35 °C) as it results from Eq. 3, the temperature dependence $D_p(T)$ is determined by the water permeability temperature dependence $P(T)$. The value of water permeability is about 0.3×10^{-5}m/s at 20 °C.

Another way of permeability calculation is the intracellular water residence time measurement.

Due to RBCs walls permeability, there is molecular exchange between intracellular, extracellular and bulk water. To calculate cell water molecules' residence time and the exchange rate constants, two-compartment model, that implies the exponential residence time distribution function, is applied. In this

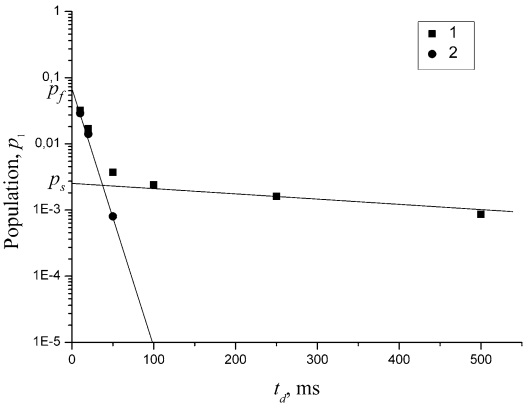

Fig. 10 *1* The dependence of intracellular water population $p_1(t_d)$ on diffusion time t_d. *2* The dependence $p_1(t_d)$ after subtraction of spin–lattice relaxation part. Temperature is 35 °C

model, the population of the compartment with the lowest self-diffusion coefficient p_1 depends on diffusion time t_d as [39, 47]

$$p_1(t_d) = p_1(0)\exp\left(-\frac{t_d}{\tau}\right) \tag{8}$$

where τ is the water molecules' residence time in the cell. This equation does not take into account the spin–lattice relaxation contribution in $p_1(t_d)$. If the spin–lattice relaxation is considered, the $p_1(t_d)$ will be biexponential according to Eq. 9 [48].

The experimental $p_1(t_d)$ dependences are well approximated by this equation.

$$p_1 = p_f \exp\left(-\frac{t_d}{\tau}\right) + p_s \exp\left(-\frac{t_d}{T_1}\right) \tag{9}$$

where τ is the residence time, T_1 is spin–lattice relaxation time, which is about 600 ms, $p_f + p_s = p_1(0)$.The estimated value of residence time is 20 ± 2 ms at 30 °C. This value is typical for RBCs residence time (Fig. 10) [20].

3.2 Blood Lipid Self-Diffusion

The diffusion decays for blood lipid component measured as echo spectra signal integral in the region 0–2 ppm at different t_d are shown in Fig. 11.

The main part of the diffusion decay belongs to the tail, which is characterized by the self-diffusion coefficient D_L, which is varied from 3×10^{-12} to 10^{-11} m^2/s depending on temperature and diffusion time. The relative part (population p_L) is increased when the echo signal integration region shifts far from water signal position. It may be concluded that the diffusion coefficient D_L characterizes the namely lateral lipid self-diffusion. The components with the larger self-diffusion coefficients which determine that the initial part of diffusion decay may belong to the wings of strong water signal.

The temperature dependence for D_L measured at diffusion time $t_d = 10$ ms is shown in Fig. 12. This dependence was approximated by Arrhenius's law. The activation energy is 25 ± 2.9 kJ/mol, which agreed well with the activation energy of model bilipid system [40].

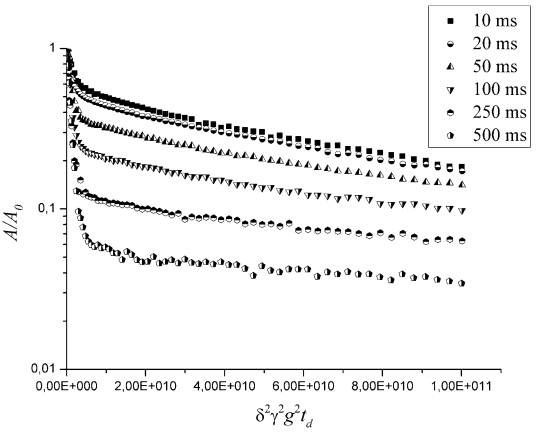

Fig. 11 The diffusion decays of integral echo signals in the region 0–2 ppm at different diffusion time t_d. The t_d values are in insertion

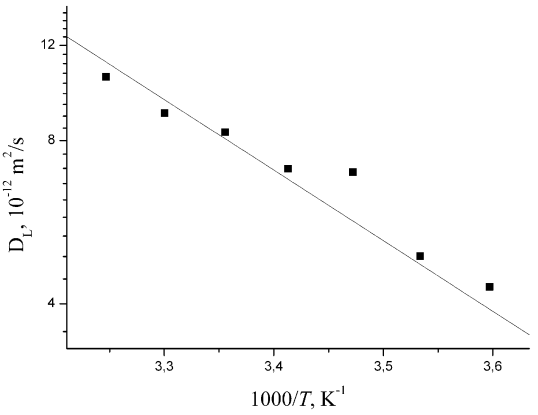

Fig. 12 The temperature dependence of lipid self-diffusion coefficients D_L. The *straight line* is the Arrhenius equation approximation. The activation energy is 25 ± 2.9 kJ/mol. The diffusion time t_d is 10 ms

The lateral self-diffusion coefficient D_{L} is decreased with increasing of diffusion time t_{d}. The dependence $D_{\mathrm{L}}(t_{\mathrm{d}})$ is shown in Fig. 13a. The effective self-diffusion coefficients $D_{\mathrm{L}}^{\mathrm{eff}}$, calculated from Eq. (7), are shown in Fig. 13b. The estimated restriction size a_L is about 1.4 μm.

4 Conclusion

The self-diffusion of water and blood lipids in mouse RBCs suspension in temperature region from 5 to 35 °C at different diffusion times was investigated by pulsed field gradient NMR technique.

The ^{1}H water molecules' diffusion decays consist of three exponential components which belong to intracellular water, extracellular water and bulk water.

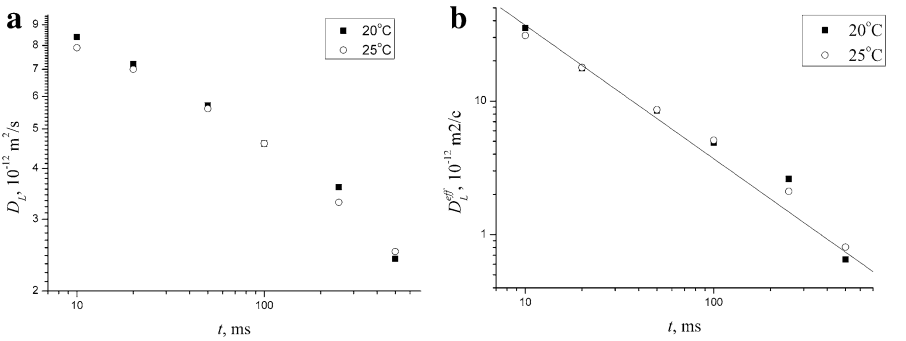

Fig. 13 **a** The dependence of the blood lipid self-diffusion coefficient $D_L(t_d)$ on diffusion time t_d at 20 and 25 °C; **b** the dependence of effective blood lipid self-diffusion coefficient D_L^{eff} (t_d) on diffusion time t_d at 20 and 25 °C, $D_p = 1.9 \times 10^{-12}$ m^2/s

The dependence of intracellular water apparent self-diffusion coefficients on diffusion time was analyzed.

The restriction size (2.1 μm) and water permeability (0.3×10^{-5} m/s) were estimated. From the temperature dependence of hindered self-diffusion coefficient D_p, the activation energy was calculated (24.1 ± 1.9 kJ/mol) which well agreed with the activation energies for other species RBCs.

The intracellular water residence time is about 20 ms, which also agreed well with literature data.

The lateral self-diffusion coefficients D_L at different temperatures and diffusion time were measured. From the temperature dependence D_L (T), the activation energy was calculated (25 ± 2.9 kJ/mol) which is in close agreement with activation energy for model lipid bilayers.

The lateral self-diffusion coefficient is also restricted. The restriction size is about 1.4 μm.

Acknowledgments The authors thank Professor Vladimir Skirda for helpful discussions.

References

1. G. Benga, S.M. Grieve, B.E. Chapman, C.H. Gallagher, P.W. Kuchel, Comp. Haemat. Int. **9**, 43 (1999)
2. G. Benga, P.W. Kuchel, B.E. Chapman, G.C. Cox, I. Ghiran, C.H. Gallagher, Comp. Haemat. Int. **10**, 1 (2000)
3. G.H. Benga, B.E. Chapman, G.C. Cox, P.W. Kuchel, Cell Biol. Int. **27**, 921 (2003)
4. T. Conlon, R. Outhred, Biochim. Biophys. Acta **288**, 354 (1972)
5. U. Himmelreich, B.E. Chapman, P.W. Kuchel, Eur. Biophys. J. **28**, 158 (1999)
6. G. Lahajnar, P. Macek, P. Smid, I. Zupancic, Biochim. Biophys. Acta **1235**, 437 (1995)
7. G. Lahajnar, P. Macek, I. Zupancic, Bioelectrochemistry **52**, 179 (2000)
8. V.V. Morariu, G. Benga, in *Membrane Processes*, ed. by G. Benga (Springer, New York, 1984), p. 121
9. G. Benga, B.E. Chapman, H. Matei, G.C. Cox, T. Romeo, E. Mironescu, P.W. Kuchel, Cell Biol. Int. **34**, 373 (2010)

10. G. Benga, B.E. Chapman, G.C. Cox, P.W. Kuchel, Cell Biol. Int. **34**, 703 (2010)
11. G. Benga, Eur. Biophys. J. **42**, 33 (2013)
12. G. Benga, B.E. Chapman, T. Romeo, G.C. Cox, P.W. Kuchel, Protoplasma **252**, 1181 (2015)
13. L.L. Latour, K. Svoboda, P.P. Mitra, C.H. Sotak, Proc. Natl. Acad. Sci. USA. Biophysics **91**, 1229 (1994)
14. A.R. Waldeck, P.W. Kuchel, A.J. Lennon, B.E. Chapman, Progr. Nucl. Magn. Reson. Spectr. **30**, 39 (1997)
15. B.E. Chapman, P.W. Kuchel, Diffusion Fundamentals 4, 8.1 (2007)
16. T.J. Larkin, P.W. Kuchel, Eur Biophys **39**, 139 (2009)
17. A.R. Waldeck, M.H. Nouri-Sorkhabi, D.R. Sullivan, P.W. Kuchel, Biophys. Chem. **55**, 197 (1995)
18. J. Andrasko, Biochimica el Biophysica Acta **428**, 304 (1976)
19. J.C. Mathai, S. Mori, B.L. Smith, G.M. Preston, N. Mohandas, M. Collinsi, P.C.M. van Zijl, M.L. Zeidel, P. Agre, J. Biol. Chem. **271**, 1309 (1996)
20. P.E. Thelwall, S.C. Grant, G.J. Stanisz, S.J. Blackband, Magn. Reson. Med. **48**, 649 (2002)
21. A.M. Torres, R.J. Michniewicz, B.E. Chapman, G.A.R. Young, P.W. Kuchel, Magn. Reson. Imaging **16**, 423 (1998)
22. A.M. Torres, A.T. Taurins, D.G. Regan, B.E. Chapman, P.W. Kuchel, J. Magn. Reson. **138**, 135 (1999)
23. C. Anselmi, F. Bernardi, M. Centini, E. Gaggelli, N. Gaggelli, D. Valensin, G. Valensin, Chem. Phys. Lipids **134**, 109 (2005)
24. G. Pages, D. Szekely, P.W. Kuchel, J. Magn. Reson. Imaging **281**, 409 (2008)
25. J.E. Tanner, E.O. Stejskal, J Chem Phys **19**, 1768 (1968)
26. A.V. Anisimov, N.Y. Sorokina, N.R. Dautova, Magn. Reson. Imaging **16**, 565 (1998)
27. K.S. Hong, G.-S. Yeom, J.-H. Cho, E.-H. Kim, C. Lee, S.D. Lee, C. Cheong, J. Korean Magn. Reson. Soc. **9**, 29 (2005)
28. A.M. Babsky, S. Topper, H. Zhang, Y. Gao, J.R. James, S.K. Hekmatyar, N. Bansal, Magn. Reson. Med. **59**, 485 (2008)
29. I. Eslund, A. Nowacka, M. Nilsson, D. Topgaard, J. Magn. Reson. **200**, 291 (2009)
30. C.-H. Cho, Y.-S. Hong, K. Kang, V.I. Volkov, V. Skirda, C.-Y.J. Lee, C.-Ho Lee. Magn. Reson. Imaging **21**, 1009 (2003)
31. Ki-J. Suh, Y.-S. Hong, V.D. Skirda, V.I. Volkov, C.-Y. Lee, C.-Ho Lee, Biophysical Chemistry 104, 121 (2003)
32. I.A. Avilova, S.G. Vasil'ev, L.V. Rimareva, E.M. Serba, L.D. Volkova, V.I. Volkov. Russ. J. Phys. Chem. A **89**, 710 (2015)
33. P.P. Mitra, P.N. Sen, L.M. Schwartz, P.L. Doussal, Phys. Rev. Lett. **68**, 3555 (1992)
34. V.V. Loskutov, J. Magn. Reson. **216**, 192 (2012)
35. V.V. Loskutov, V.A. Sevriugin, J. Magn. Reson. **230**, 1 (2013)
36. R.R. Valiullin, V.D. Skirda, S. Stapf, R. Kimmich R. Phys. Rev. E **55**, 2664 (1996)
37. J. Karger and D. M. Ruthven, Diffusion in Zeolites and Other Microporous Solids, John Wiley, New York, USA (1992). 605 p
38. P.T. Callaghan, *Principle of NMR Microscopy* (Clarenden Press, Oxford, 1991), p. 492
39. A.I. Maklakov, V.D. Skirda, N.F. Fatkullin. Self-Diffusion in Polymer Solutions and Melts. Kazan: Kazan State University Press, 1987 (in Russian), p. 223
40. A. Filippov, G. Oradd, G. Lindblom, Biophys. J. **84**, 3079 (2003)
41. E.Yu.Tchashkova, V.G.Gorokhov, E.E.Kuznetsova, N.S.Korotaeva, E.G.Grigoriev, V.E.Pak, R.F.Barakov. Experimental & clinical gastroenterology) 5, 21 (2009) **(in Russian)**
42. V.I. Volkov, S.A. Korotchkova, H. Ohya, Q. Guo, J. Membr. Science **100**, 273 (1995)
43. A.V. Anisimov, N.Y. Sorokina, N.R. Dautova, Magn. Reson. Im. **16**, 565 (1998)
44. P.P. Mitra, P.N. Sen, L.M. Schawartz, Phys. Rev. B **47**, 8565 (1993)
45. R.R. Valiullin, V.D. Skirda, J. Chem, Phys. **114**, 452 (2001)
46. V.V. Loskutov, E.P. Petrov, Appl. Magn. Reson. **45**, 1389 (2014)
47. J. Karger, H. Pheifer, W. Heink, in *Principles and application of self-diffusion measurements by nuclear magnetic resonance*, vol. 12, ed. by J.S. Waugh (Academic Press, New York, 1988), p. 1
48. Y.S. Hong, K.C. Kim, V.I. Volkov, V.D. Skirda, C.-H. Lee, Appl. Magn. Reson. **29**, 351 (2005)